Impact of Antarctic Circumpolar Current Development on Late Paleogene Ocean Structure

Miriam E. Katz, *et al.*

Science **332**, 1076 (2011);
DOI: 10.1126/science.1202122

10. J. S. Kim, C. O. Pabo, *Proc. Natl. Acad. Sci. U.S.A.* **95**, 2812 (1998).
11. D. L. Masica, S. B. Schrier, E. A. Specht, J. J. Gray, *J. Am. Chem. Soc.* **132**, 12252 (2010).
12. D. Röthlisberger *et al.*, *Nature* **453**, 190 (2008).
13. L. Jiang *et al.*, *Science* **319**, 1387 (2008).
14. D. Häring, M. D. Distefano, *Bioconjug. Chem.* **12**, 385 (2001).
15. J. Kaplan, W. F. DeGrado, *Proc. Natl. Acad. Sci. U.S.A.* **101**, 11566 (2004).
16. R. Fairman, K. S. Akerfeldt, *Curr. Opin. Struct. Biol.* **15**, 453 (2005).
17. W. F. DeGrado, J. D. Lear, *J. Am. Chem. Soc.* **107**, 7684 (1985).
18. S. Segman, M. R. Lee, V. Vaiser, S. H. Gellman, H. Rapaport, *Angew. Chem. Int. Ed. Engl.* **49**, 716 (2010).
19. H. Rapaport, *Supramol. Chem.* **18**, 445 (2006).
20. M. Zheng *et al.*, *Science* **302**, 1545 (2003).
21. X. Tu, S. Manohar, A. Jagota, M. Zheng, *Nature* **460**, 250 (2009).
22. S. Wang *et al.*, *Nat. Mater.* **2**, 196 (2003).
23. G. R. Dieckmann *et al.*, *J. Am. Chem. Soc.* **125**, 1770 (2003).
24. A. Ortiz-Acevedo *et al.*, *J. Am. Chem. Soc.* **127**, 9512 (2005).
25. E. Katz, I. Willner, *ChemPhysChem* **5**, 1084 (2004).
26. G. Grigoryan, W. F. DeGrado, *J. Mol. Biol.* **405**, 1079 (2011).
27. Materials and methods are available as supporting material on *Science* Online.
28. G. Ghirlanda, J. D. Lear, N. L. Ogihara, D. Eisenberg, W. F. DeGrado, *J. Mol. Biol.* **319**, 243 (2002).
29. L. A. Capriotti, T. P. Beebe Jr., J. P. Schneider, *J. Am. Chem. Soc.* **129**, 5281 (2007).
30. P. Nygren, M. Lundqvist, K. Broo, B. H. Jonsson, *Nano Lett.* **8**, 1844 (2008).
31. M. J. O'Connell *et al.*, *Science* **297**, 593 (2002).
32. O. N. Torrens, D. E. Milkie, M. Zheng, J. M. Kikkawa, *Nano Lett.* **6**, 2864 (2006).
33. D. Golberg, Y. Bando, C. C. Tang, C. Y. Zhi, *Adv. Mater. (Deerfield Beach Fla.)* **19**, 2413 (2007).
34. A. K. Chakraborty, A. J. Golumbfskie, *Annu. Rev. Phys. Chem.* **52**, 537 (2001).
35. G. E. Crooks, G. Hon, J. M. Chandonia, S. E. Brenner, *Genome Res.* **14**, 1188 (2004).

Acknowledgments: This work was supported by the NSF Materials Research Science and Engineering Center DMR05-20020 grant (to J.M.K., M.D., and W.F.D.), NIH grant no. GM54616 (to W.F.D.), a NSF National Science and Engineering Center grant no. DMR-0425780 (to W.F.D. and M.D.), NSF grant no. DMR-0907226 (to J.M.K.), and NIH grant no. 5F32GM084631-02 (to G.G.). K.A. acknowledges support from the Roy and Diana Vagelos Program in the Molecular Life Sciences, and L.W. acknowledges funding from the NSF–Integrative Graduate Education and Research Traineeship program (grant DGE-0221664). We would like to thank K. A. McAllister for training Y.H.K. in peptide synthesis, and A. E. Keating for comments on the manuscript.

Supporting Online Material
www.sciencemag.org/cgi/content/full/332/6033/1071/DC1
Materials and Methods
Figs. S1 to S15
Tables S1 to S3
References (*26*, *36*–*61*)

8 October 2010; accepted 13 April 2011
10.1126/science.1198841

Impact of Antarctic Circumpolar Current Development on Late Paleogene Ocean Structure

Miriam E. Katz,[1]* Benjamin S. Cramer,[2] J. R. Toggweiler,[3] Gar Esmay,[4] Chengjie Liu,[5] Kenneth G. Miller,[4] Yair Rosenthal,[4,6] Bridget S. Wade,[7] James D. Wright[4]

Global cooling and the development of continental-scale Antarctic glaciation occurred in the late middle Eocene to early Oligocene (~38 to 28 million years ago), accompanied by deep-ocean reorganization attributed to gradual Antarctic Circumpolar Current (ACC) development. Our benthic foraminiferal stable isotope comparisons show that a large $\delta^{13}C$ offset developed between mid-depth (~600 meters) and deep (>1000 meters) western North Atlantic waters in the early Oligocene, indicating the development of intermediate-depth $\delta^{13}C$ and O_2 minima closely linked in the modern ocean to northward incursion of Antarctic Intermediate Water. At the same time, the ocean's coldest waters became restricted to south of the ACC, probably forming a bottom-ocean layer, as in the modern ocean. We show that the modern four-layer ocean structure (surface, intermediate, deep, and bottom waters) developed during the early Oligocene as a consequence of the ACC.

The Antarctic Circumpolar Current (ACC) is a dominant feature of present-day ocean circulation and climate, influencing the strength of meridional overturning circulation, transition depth from surface to deep ocean, gas-exchange rate between atmosphere and deep ocean, and global surface heat distribution (*1*–*4*). Wind-driven ACC upwelling is the major mode of water transport from the ocean interior to the surface, setting the density structure for the ocean interior from the Southern Ocean to high northern latitudes (*5*). The ACC also stabilizes asymmetrical meridional overturning circulation, with more-dense southern-sourced water constrained to bottom depths below the ACC (>2500 m) and overlain by northern-sourced deep waters (Fig. 1).

The ACC "engine" began to develop in the middle Eocene with shallow flow through the Drake Passage between Antarctica and South America (*6*, *7*), followed by rapid deepening of the Tasman gateway between Antarctica and Australia from the late Eocene to early Oligocene (*8*, *9*) and more-gradual deepening of the Drake Passage through the remainder of the Oligocene (*7*) (Fig. 1). It has been proposed that the modern characteristics of the ACC and its effects on deepwater circulation did not develop until the late Oligocene (*9*–*12*). However, a persistent difference in Southern Ocean benthic foraminiferal $\delta^{18}O$ values relative to those of the Pacific and North Atlantic that developed by the early Oligocene did not require a deep ACC; shallow-depth ACC circulation is sufficient for thermal isolation of the high-latitude Southern Ocean from warm surface subtropical gyres (*1*–*4*, *13*), with the potential to affect deepwater source regions. Changes in benthic and planktonic microfossil communities (*14*, *15*), North Atlantic and Pacific drift accumulation (*16*, *17*), and erosional hiatuses in the deep ocean (*18*) support the idea that gradual deep ocean changes occurred through the middle Eocene to late Oligocene.

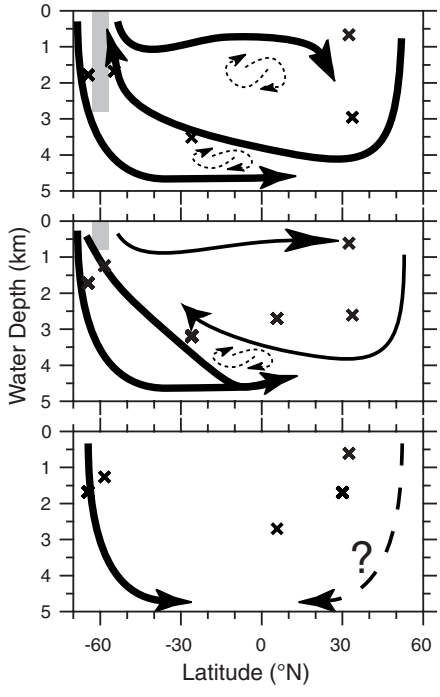

Fig. 1. Effect of progressive ACC deepening on water masses. X's indicate the paleodepths of isotopic records used to reconstruct Eocene-Oligocene water masses in this study. (**Bottom**) No ACC, analogous to pre–mid-Eocene; SCW dominates the deep ocean. (**Middle**) A multilayer ocean begins to develop with a shallow ACC, analogous to the early Oligocene. (**Top**) Multilayer modern ocean with deep ACC, analogous to the late Oligocene to the present.

[1]Department of Earth and Environmental Sciences, Rensselaer Polytechnic Institute, Troy, NY 12180, USA. [2]Theiss Research, Eugene, OR, USA. [3]Geophysical Fluid Dynamics Lab/National Oceanic and Atmospheric Administration, Princeton, NJ, USA. [4]Department of Earth and Planetary Sciences, Rutgers University, Piscataway, NJ 08854, USA. [5]ExxonMobil Exploration, Post Office Box 4778, Houston, TX 77210-4778, USA. [6]Institute of Marine and Coastal Sciences, Rutgers University, New Brunswick, NJ 08901, USA. [7]School of Earth and Environment, University of Leeds, Leeds LS2 9JT, UK.

*To whom correspondence and requests for materials should be addressed. E-mail: katzm@rpi.edu

Although Oligocene isotopic patterns and interbasinal gradients are well documented for deepwater locations (*13*), little is known about intermediate-water evolution during this time of large-scale circulation changes. Intermediate-water circulation today is a consequence of the ACC, which blocks warm surface waters entrained in subtropical gyres from reaching Antarctica; this thermally isolates the continent and the surrounding ocean, allowing large-scale ice sheets to persist. At the boundary between the eastward-flowing ACC and westward-flowing Antarctic Coastal Current, Ekman divergence leads to substantial upwelling of deep water, which is then replaced by the formation of Antarctic Bottom Water (AABW) and North Atlantic Deep Water (NADW). The AABW circulation cell is closed by AABW mixing into NADW and locally recirculated water that upwells at the ACC. The NADW circulation cell is closed by the northward flow of nutrient-rich Antarctic Intermediate Water (AAIW) that feeds the downwelling in the North Atlantic. In the warmer Oligocene ocean, North Pacific deepwater formation should have been at least as strong as in the North Atlantic (*19*) and may have mixed similarly with southern-sourced waters. NADW and AAIW strength and the NADW-AABW boundary are therefore strongly affected by the strength and depth of the ACC.

We provide direct evidence to constrain intermediate-water development associated with the evolution of the ACC in the late Eocene to early Miocene. We present benthic foraminiferal isotopes with Mg/Ca data from two North American Atlantic continental slope locations (Fig. 2) with well-preserved foraminifera and excellent age control (figs. S1 and S2 and tables S1 to S3), providing a continuous record from the late middle Eocene to early Miocene: (i) Ocean Drilling Program (ODP) Site 1053 (Blake Nose, 1629 m present depth, ~1500 to 1750 m paleodepth); and (ii) Atlantic Slope Project corehole 5 (ASP-5; 250 m present depth, 600 m paleodepth, North Carolina slope) (table S4).

Global oxygen isotope events recorded at ASP-5 (such as Oi-1, Oi-2, Oi-2a, Oi-2b, and Mi-1) and the Mg/Ca-inferred cooling associated with Oi-1 (Fig. 2) support the validity of our age model. Our Site 1053 data fill the late Eocene hiatus at ASP-5, providing context for the inter- and intrabasinal $\delta^{13}C$ changes observed in the Oligocene (Fig. 2). There is no clear distinction among $\delta^{13}C$ values at ASP-5, Site 1053, and the deep North Atlantic during the Eocene. ASP-5 $\delta^{18}O$ values are lower than those in the deeper North Atlantic, including Site 1053, reflecting warmer temperatures at shallower paleodepths.

The abrupt growth of continent-scale Antarctic ice sheets in the earliest Oligocene is reflected in the global >1 per mil (‰) increase in benthic foraminiferal $\delta^{18}O$ (called Oi-1) (*20*, *21*). At ASP-5, a 1.1‰ increase culminates in Oi-1, whereas Mg/Ca indicates a ~2.5°C cooling, suggesting that about half of the $\delta^{18}O$ increase was due to ice-sheet growth (Fig. 2). This is consistent with records from two shallow-water locations (*22*, *23*) free of carbonate saturation issues that may bias deepwater Mg/Ca temperature estimates. The ASP-5 ~2.5°C cooling is the first from a mid-depth location; it is generally assumed that the deep-ocean $\delta^{18}O$ increase also partly reflects a cooling, but the large change in deep-ocean carbonate saturation has prevented a direct estimate of the magnitude (*24*).

Coincident with Oi-1, a >0.5‰ difference developed between benthic foraminiferal $\delta^{18}O$ values from the Southern Ocean and South Atlantic relative to values from the North Atlantic and Pacific (Fig. 3), in contrast to the lack of statistically significant interbasinal offsets throughout the Paleocene to middle Eocene (*13*). This early Oligocene isotopic differentiation indicates a temperature difference similar to the ~2°C difference between modern northern- and southern-sourced deep water; therefore, analogous to modern ocean structure, early Oligocene isotopic differentiation reflects proto-ACC intensification through the Drake Passage (*13*) (Fig. 1).

Unlike the significant $\delta^{18}O$ offsets, deepwater interbasinal $\delta^{13}C$ gradients remained low in the Oligocene, consistent with Eocene gradients (*13*, *25*, *26*) (Fig. 3). In contrast, a ~1.2‰ $\delta^{13}C$ offset developed between ASP-5 and deepwater sites in all basins by ~30 to 31 million years ago (Ma) and persisted across Mi-1 into the early Miocene (Fig. 3). This $\delta^{13}C$ offset indicates greater oxidation of organic matter at ASP-5, at a time when a stable Gulf Stream (*27*) was unlikely to account for the $\delta^{13}C$ decrease at ASP-5. In the modern North Atlantic, the vertical $\delta^{13}C$ gradient between deep and intermediate waters is <0.5‰. In contrast, the larger Oligocene vertical $\delta^{13}C$ gradient is analogous to the modern Pacific gradient (fig. S3).

In the modern ocean, AAIW that forms along the northern edge of the ACC (Fig. 1) keeps the thermocline ventilated to ~700 to 1000 m in the Atlantic and Pacific and sets the depth of the low-O_2 layer (relative to surrounding waters), although this depth can vary along the continental slope (*28*) (fig. S3). This low-O_2 layer typically lies just below the salinity minimum, which itself marks the limit of AAIW ventilation (*28*). The oxidation of organic matter in the surface ocean and low ventilation rates in the deep ocean lead to a rapid reduction in oxygenation with depth through the upper few hundred meters of the water column. The depth of the modern low-O_2 layer is set primarily by a decrease in ventilation at the lower boundary of AAIW. Therefore, ventilation by AAIW leads to a relatively deep low-O_2 and low-$\delta^{13}C$ layer (~700 to 1000 m).

In the absence of a mode water similar to modern AAIW, high O_2 consumption rates near the surface would result in a much shallower low-O_2 and low-$\delta^{13}C$ layer. This appears to have been the case during the Eocene, when $\delta^{13}C$ values at 600 m (ASP-5) were similar to those in the deep ocean as a result of rapid oxidation of organic matter shallower than ASP-5. With expansion to northern mid-latitudes (ASP-5),

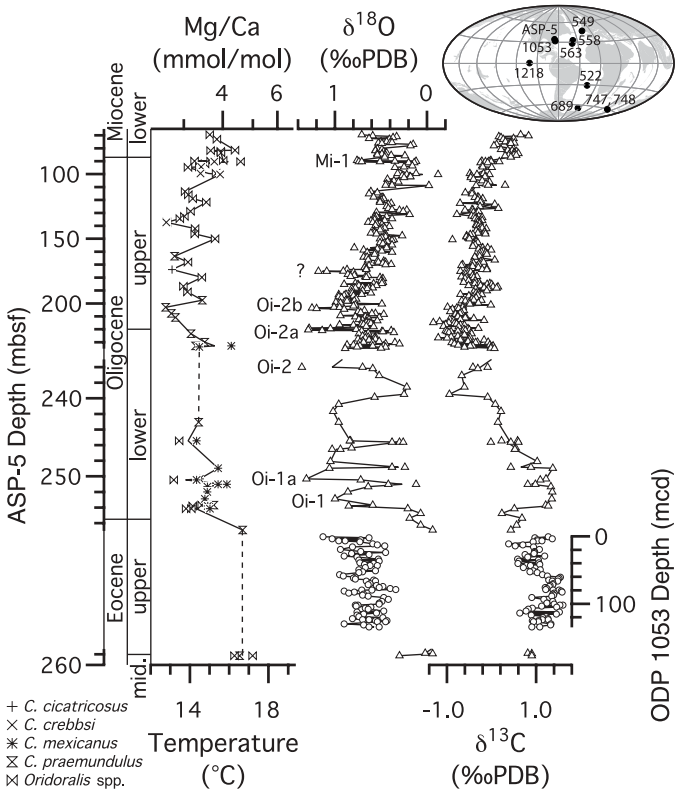

Fig. 2. Location map inset into analyses of benthic foraminiferal (*Cibicidoides* spp.) $\delta^{18}O$ and $\delta^{13}C$ values from ASP-5 (triangles) and Site 1053 (circles) and Mg/Ca values from ASP-5 (*Cibicidoides* and *Oridorsalis* species, symbol key provided). The traces pass through the mean value for samples with multiple analyses. The ASP-5 depth axis is split according to age model so that the equivalent age scale is approximately linear; the Site 1053 record is inserted within an ASP-5 hiatus. The temperature (T) axis is calculated using Mg/Ca = 1.528 exp(0.09 T) (*36*) and is scaled to match the range of the $\delta^{18}O$ axis, using $T = 16.1 - 4.64(\delta^{18}O_{bf} - \delta^{18}O_{sw}) + 0.09(\delta^{18}O_{bf} - \delta^{18}O_{sw})^2$ [quadratic approximation by (*37*) to relationship found by (*38*)] (bf, benthic foraminifera; sw, seawater). No correction was applied for genus/species offsets in the Mg/Ca record. PDB, Pee Dee belemnite values.

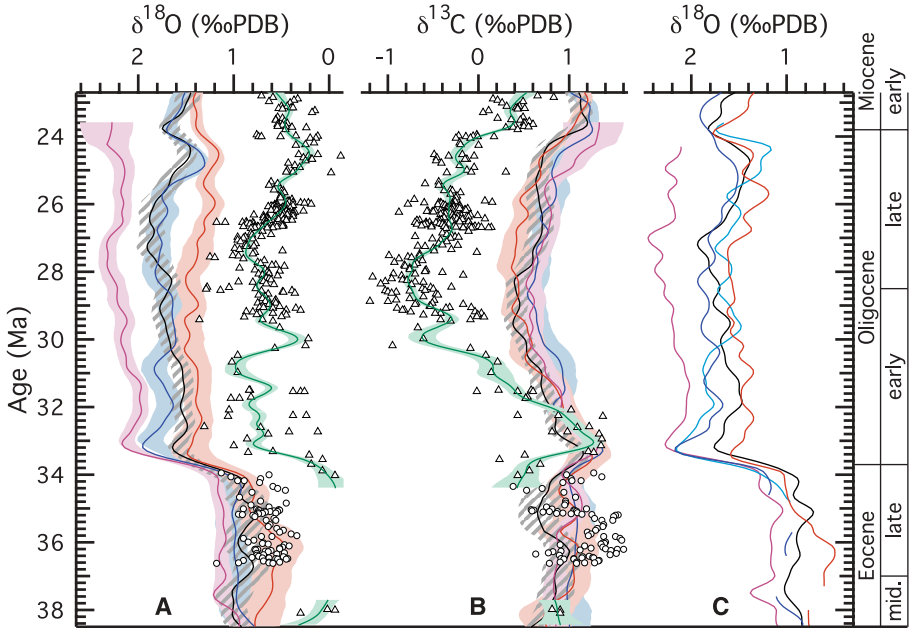

Fig. 3. Comparison of stable isotopic data with trend lines from ASP-5 and ODP Site 1053 (green) with deep-ocean stable isotope trends from (*13*) (A, $\delta^{18}O$; B, $\delta^{13}C$). Locations are indicated as follows: Pacific (gray slashes), North/Equatorial Atlantic (red), South Atlantic/sub-Antarctic (blue), and high-latitude Southern (purple). Data trends were calculated using a LOESS smoothing with 0.8-million-year window. A color band indicates the 95% confidence level for trend estimates. The $\delta^{13}C$ offset between ASP-5 and the deep basins between Oi-1 and the hiatus (~33.5 to 34 Ma) indicates that using $\delta^{13}C$ stratigraphy in this short interval would improve our age model. We do not do this because the $\delta^{13}C$ records are the main focus of our paper and therefore cannot be used in the age model. C: Sub-Antarctic $\delta^{18}O$ values shift away from Southern Ocean values toward North Atlantic values beginning ~31 to 30 Ma. Locations are indicated as follows: Southern Ocean Site 689 (purple); sub-Antarctic Site 748 (>~25 Ma) and Site 747 (<~25 Ma) (dark blue); South Atlantic Site 522 (light blue); Pacific Site 1218 (black); and North Atlantic Site 549 (>~25 Ma), Site 558 (<~34 Ma), and Site 563 (<~33 Ma) (red). Data are compiled in (*13*). See Fig. 2 for locations.

better-oxygenated intermediate waters oxidized more organic matter, released ^{12}C, and drove benthic foraminiferal $\delta^{13}C$ to lower values, similar to modern AAIW ventilation of the Pacific. However, the $\delta^{13}C$ offset between ASP-5 and the deep North Atlantic was larger in the Oligocene than in the modern Pacific, and therefore the offset may reflect higher $\delta^{13}C$ in the Oligocene deep ocean relative to intermediate waters. This difference may be attributed to deep Atlantic waters that were younger in the Oligocene than deep Pacific waters are today.

Strengthening and deepening of the ACC in the early Oligocene would have enhanced the formation of southern-sourced intermediate water (via downwelling at the northern edge of the ACC); this is recorded in the decreasing $\delta^{13}C$ values at ASP-5 at ~31 to 30 Ma. In addition, changes in the ACC would have restricted the coldest water to below the ACC and allowed the incursion of northern-component water (NCW, analogous to NADW) progressively farther south in the Atlantic (Fig. 1), resulting in the shift of $\delta^{18}O$ values at South Atlantic Site 522 away from colder Southern Ocean values and toward the warmer North Atlantic values (Fig. 3). The gradual confinement of southern-component water (SCW) by the ACC occurred over several million years; $\delta^{18}O$ values at sub-Antarctic Sites 747 and 748 remained closer to those in the high-latitude Southern Ocean than in the Pacific for ~3 million years after the $\delta^{18}O$ decrease at lower-latitude Site 522 and $\delta^{13}C$ decrease at ASP-5 (Fig. 3). Together, these early isotopic changes indicate that the modern four-layer ocean structure (surface, intermediate, deep, and bottom waters) first developed during the early Oligocene (Figs. 1 and 3).

At the same time, early Oligocene subsidence of the Greenland-Scotland Ridge (GSR) facilitated NCW production in the Norwegian-Greenland Sea (*29*, *30*). GSR subsidence continued to its greatest depth (240 to 320 m) at ~31 Ma (*29*). Decreasing εNd values support increased NCW flow at this time (*31*–*33*). ASP-5 isotope records indicate an early Oligocene transition in the mid-depth western North Atlantic, before a fully opened Drake Passage and deep ACC, which is consistent with models that predict that a shallow-depth ACC would affect thermocline waters throughout the Atlantic (*2*). This predates initial uplift of the Isthmus of Panama by at least 15 million years (*34*, *35*), precluding any impact on changing intermediate waters in the Oligocene North Atlantic. We speculate that southern-sourced intermediate water, enhanced by the developing ACC, facilitated NCW production as the GSR subsided and the Drake Passage and Tasman Rise continued to open (Figs. 1 and 3).

The evolution of deep and intermediate water circulation and the ACC beginning in the latter part of the Eocene corresponds to the "doubthouse climate" interval: the transition from early Paleogene greenhouse climates to the icehouse climates that have dominated the rest of the Cenozoic. Our Atlantic slope data and inter- and intrabasinal isotopic comparisons indicate that ocean thermal structure and circulation were affected at an early stage of opening of the Drake Passage. Our results indicate that changes in tectonic gateways affected late middle Eocene to early Miocene ocean circulation, which in turn affected global climate.

References and Notes

1. M. D. Cox, *J. Phys. Oceanogr.* **19**, 1730 (1989).
2. J. R. Toggweiler, H. Bjornsson, *J. Quat. Sci.* **15**, 319 (2000).
3. W. P. Sijp, M. H. England, *J. Clim.* **18**, 1957 (2005).
4. W. P. Sijp, M. H. England, *J. Phys. Oceanogr.* **34**, 1254 (2004).
5. J. R. Toggweiler, B. Samuels, *J. Phys. Oceanogr.* **28**, 1832 (1998).
6. H. D. Scher, E. E. Martin, *Science* **312**, 428 (2006).
7. R. Livermore, C.-D. Hillenbrand, M. Meredith, G. Eagles, *Geochem. Geophys. Geosyst.* **8**, Q01005 (2007).
8. N. Exon, J. Kennett, M. Malone, in *Proceedings of the Ocean Drilling Program, Scientific Results*, N. Exon, J. Kennett, M. Malone, Eds. (ODP, College Station TX, 2004), vol. 189, pp. 1–37.
9. C. E. Stickley *et al.*, *Paleoceanography* **19**, PA4027 (2004).
10. P. F. Barker, E. Thomas, *Earth Sci. Rev.* **66**, 143 (2004).
11. H. A. Pfuhl, I. N. McCave, *Earth Planet. Sci. Lett.* **235**, 715 (2005).
12. M. Lyle, S. Gibbs, T. C. Moore, D. K. Rea, *Geology* **35**, 691 (2007).
13. B. S. Cramer, J. R. Toggweiler, J. D. Wright, M. E. Katz, K. G. Miller, *Paleoceanography* **24**, PA4216 (2009).
14. M. E. Katz, R. C. Tjalsma, K. G. Miller, *Micropaleontology* **49** (suppl. 2), 1 (2003).
15. M.-P. Aubry, D. Bord, in *The Late Eocene Earth—Hothouse, Icehouse, and Impacts*, C. Koeberl, A. Montanari, Eds. (Geological Society of America, Denver, CO, 2009), Geological Society of America Special Paper 452, pp. 279–301.
16. C. N. Wold, *Paleoceanography* **9**, 917 (1994).
17. D. K. Rea, I. A. Basov, L. A. Krissek, L. S. Party, in *Proceedings of the Ocean Drilling Program, Scientific Results*, D. Rea, L. Basov, D. Scholl, J. Allan, Eds. (ODP, College Station, TX, 1995), vol. 145, pp. 577–596.
18. J. D. Wright, K. G. Miller, in *The Antarctic Paleoenvironment: A Perspective on Global Change*, J. P. Kennett, D. A. Warnke, Eds. (American Geophysical Union, Washington, DC, 1993), vol. 56, pp. 1–25.
19. A. M. de Boer, J. R. Toggweiler, D. M. Sigman, *J. Phys. Oceanogr.* **38**, 435 (2008).
20. K. G. Miller *et al.*, *Science* **310**, 1293 (2005).
21. K. G. Miller, J. D. Wright, R. G. Fairbanks, *J. Geophys. Res.* **96**, 6829 (1991).
22. M. E. Katz *et al.*, *Nat. Geosci.* **1**, 329 (2008).
23. C. H. Lear, T. R. Bailey, P. N. Pearson, H. K. Coxall, Y. Rosenthal, *Geology* **36**, 251 (2008).
24. C. Lear, R. Rosenthal, *Geology* **34**, 985 (2006).
25. K. G. Miller, R. G. Fairbanks, in *The Carbon Cycle and Atmospheric CO_2: Natural Variations Archean to Present*, E. T. Sundquist, W. S. Broecker, Eds. (American Geophysical Union, Washington DC, 1985), pp. 469–486.
26. L. Diester-Haass, J. Zachos, in *From Greenhouse to Icehouse; the Marine Eocene-Oligocene Transition*, D. R. Prothero, L. C. Ivany, E. A. Nesbitt, Eds. (Columbia Univ. Press, New York, 2003), pp. 397–416.
27. P. R. Pinet, P. Popenoe, *Geol. Soc. Am. Bull.* **96**, 618 (1985).
28. L. D. Talley, in *The South Atlantic: Present and Past Circulation*, G. Wefer, W. H. Berger, G. Siedler, D. J. Webb, Eds. (Springer-Verlag, Berlin, 1996), pp. 219–238.
29. M. Abelson, A. Agnon, A. Almogi-Labin, *Earth Planet. Sci. Lett.* **265**, 33 (2008).

30. J. D. Wright, K. G. Miller, *Paleoceanography* **11**, 157 (1996).
31. H. D. Scher, E. E. Martin, *Paleoceanography* **23**, PA1205 (2008).
32. H. D. Scher, E. E. Martin, *Earth Planet. Sci. Lett.* **228**, 391 (2004).
33. R. K. Via, D. J. Thomas, *Geology* **34**, 441 (2006).
34. G. H. Haug, R. Tiedemann, *Nature* **393**, 673 (1998).
35. E. E. Martin, B. A. Haley, *Geochim. Cosmochim. Acta* **64**, 835 (2000).
36. M. Raitzsch, H. Kuhnert, J. Groeneveld, T. Bickert, *Geochem. Geophys. Geosyst.* **9**, Q05010 (2008).
37. B. E. Bemis, H. J. Spero, J. Bijma, D. W. Lea, *Paleoceanography* **13**, 150 (1998).
38. S.-T. Kim, J. R. O'Neil, *Geochim. Cosmochim. Acta* **61**, 3461 (1997).

Acknowledgments: This research was supported by NSF grants OCE 06-23256 (M.E.K., K.G.M., B.S.W., and J.D.W.), OCE 09-28607 (B.S.C. and M.E.K.), EAR03-07112 (K.G.M.), and EAR05-06720 (K.G.M.). This research used samples provided by the ODP, which is sponsored by NSF and participating countries under management of the Joint Oceanographic Institutions, Inc. The authors declare that they have no competing financial interests.

Supporting Online Material

www.sciencemag.org/cgi/content/full/332/6033/1076/DC1
Methods
SOM Text
Figs. S1 to S3
Tables S1 to S4
References

23 December 2010; accepted 13 April 2011
10.1126/science.1202122

Early Warnings of Regime Shifts: A Whole-Ecosystem Experiment

S. R. Carpenter,[1]* J. J. Cole,[2] M. L. Pace,[3] R. Batt,[1] W. A. Brock,[4] T. Cline,[1] J. Coloso,[3] J. R. Hodgson,[5] J. F. Kitchell,[1] D. A. Seekell,[3] L. Smith,[1] B. Weidel[1]

Catastrophic ecological regime shifts may be announced in advance by statistical early warning signals such as slowing return rates from perturbation and rising variance. The theoretical background for these indicators is rich, but real-world tests are rare, especially for whole ecosystems. We tested the hypothesis that these statistics would be early warning signals for an experimentally induced regime shift in an aquatic food web. We gradually added top predators to a lake over 3 years to destabilize its food web. An adjacent lake was monitored simultaneously as a reference ecosystem. Warning signals of a regime shift were evident in the manipulated lake during reorganization of the food web more than a year before the food web transition was complete, corroborating theory for leading indicators of ecological regime shifts.

Massive ecosystem changes affect water supplies, fisheries, productivity of rangelands and forests, and other ecosystem services (*1*, *2*). Nonlinear regime shifts often come as surprises. However, recent research has revealed statistical signals that precede some nonlinear transitions, such as rising autocorrelation, steep increases in variance, and extreme changes in skewness and shift in variance spectra toward low frequencies (*3*–*7*). If the transition is approached slowly and the right variables are sampled frequently, warnings may be evident well before the regime shift is complete. Empirical evidence for early warnings of environmental regime shifts comes from a time series of major changes in paleoclimate (*8*), spatial pattern of dryland vegetation during desertification (*9*), variability of exploited fisheries (*10*, *11*), and laboratory studies (*12*). Here, we present a test of early warning indicators from a large-scale multiyear field experiment using a manipulated and a reference ecosystem.

Gradual addition or removal of top predators destabilizes food webs, and extreme manipulations of predators cause trophic cascades, a type of regime shift that alters food web structure and ecosystem processes such as primary production, ecosystem respiration, and nutrient cycling (*13*, *14*). Predator-driven transitions in lakes involve nonlinear dynamics of fish, zooplankton, and phytoplankton populations (*15*). Over 3 years, we gradually added a top predator, largemouth bass (*Micropterus salmoides*), to a lake dominated by planktivorous fishes to destabilize the food web and induce a trophic cascade leading to dominance of the food web by piscivores (*16*). A nearby lake, dominated by adult largemouth bass, was not manipulated and served as a reference ecosystem. The reference ecosystem allows us to evaluate the possibility that responses were caused by external drivers rather than the manipulation (*15*). Planktivorous fishes, zooplankton, and phytoplankton were monitored daily in both lakes for 3 years of summer stratification (2008 to 2010) (*16*).

Predicted responses of the food web follow from previous experiments in these lakes (*15*) and an ecosystem model calibrated for the manipulated lake (*17*). Before manipulation, the manipulated ecosystem was dominated by a variety of small fishes [hereafter planktivores (*16*)], and largemouth bass were few. We expected that the addition of largemouth bass would trigger recruitment of juvenile bass that were planktivorous initially but became omnivorous, adding benthos and fish to their diets, as they grew. Piscivory by largemouth bass would cause planktivorous fishes to seek refuge from predation by occupying littoral refugia and shoaling (aggregating). Eventually piscivory would drive planktivorous fishes to low densities. As planktivory declined in the open water, larger-bodied zooplankton (including migratory *Daphnia pulex*) would increase in relative abundance. Increased grazing would lead to cyclic oscillations of zooplankton and phytoplankton biomass. Thus, the food web transition would exhibit a sequence of nonlinear changes resulting from shoaling and diel movements of consumers, species replacement, and predator-prey cycles as the manipulated ecosystem became more similar to the reference ecosystem. We hypothesized that dynamics during this transitional period would generate early warning signals of a regime shift toward a piscivore-dominated food web.

Transitional dynamics of the food web were consistent with our expectations (Fig. 1). In the manipulated lake, 39 adult largemouth bass were present at the beginning of the experiment. We added 12 largemouth bass on day 193 of 2008, and 15 largemouth bass on each of days 169 and 203 of 2009. Enhancement of adult largemouth bass triggered a recruitment event in 2009, leading to 1281 young-of-year largemouth bass (95% confidence interval of 1088 to 1560) by day 240 of 2009. Numbers of this cohort (1+ in Fig. 1C) declined through 2010, whereas surviving individuals grew in body mass and became piscivorous. Planktivore numbers in the manipulated lake declined through the study as piscivory increased and were similar to those of the reference lake by about day 230 of 2010 (Fig. 1F).

The spatial pattern of planktivores was occasionally patchy in 2008 and 2009, indicated by high values in the discrete Fourier transform (DFT) of spatial data (*16*, *18*) (Fig. 2). Patchy distributions were more frequent and of longer duration in 2010. Patchy distributions indicate shoaling behavior, a likely response to predation risk.

Zooplankton biomass of the manipulated lake declined during the summers of 2008 and 2009 and became strongly oscillatory in 2010 (Fig. 1). Through 2009 and 2010, dominance of the zooplankton shifted toward larger-bodied cladocerans, including *D. pulex*, in the manipulated lake (fig. S1), consistent with previous whole-lake experiments in which body size but not biomass of zooplankton responded to fish manipulations (*15*, *19*). Phytoplankton biomass as measured by chlorophyll a of the manipulated lake displayed strong oscillations in 2009 and the first half of 2010. By day 230 of 2010, manipulated and reference lakes were similar in planktivore numbers, zooplankton biomass, and chlorophyll.

Modeling predicts that early warning indicators would appear after the largemouth bass addition in 2008 and continue until stabilization of a new food web dominated by largemouth bass

[1]Center for Limnology, University of Wisconsin, Madison, WI 53706, USA. [2]Cary Institute of Ecosystem Studies, Millbrook, NY 12545, USA. [3]Department of Environmental Sciences, University of Virginia, Charlottesville, VA 22904, USA. [4]Department of Economics, University of Wisconsin, Madison, WI 53706, USA. [5]Department of Biology, St. Norbert College, De Pere, WI 54115, USA.

*To whom correspondence should be addressed. E-mail: srcarpen@wisc.edu